*Journal of Imaging Science and Technology*® 61(4): 040406-1–040406-7, 2017.


# Video Magnification for Biomedical Dynamic Images Using Separation of the Chromophore Component

**Munenori Fukunishi▲, Kouki Kurita, and Norimichi Tsumura▲**
*Graduate School of Advanced Integration Science, Chiba University, Chiba, Japan*
*E-mail: fukunishi.m@gmail.com*

**Abstract.** *In this article, the authors propose a novel method of video magnification based on separation of the chromophore component. A video magnification method, Eulerian video magnification, was originally proposed by Wu et al. The method is effective in amplifying slight changes of facial color and can visualize the blood flow in the human face effectively. However, the conventional method was evaluated under stable conditions of illumination. It is necessary to enhance its robustness against environmental change for practical use. The proposed method amplifies the variation of the chromophore component which is separated from the shading component. The authors confirm that the proposed method can visualize the blood flow in the human face without artifacts caused by shading change. They also apply the video magnification framework to a tongue movie as preliminary work for medical application and confirm its effectiveness in visualizing the blood pulse and avoiding any clear artifacts.* © *2017 Society for Imaging Science and Technology.*
[DOI: 10.2352/J.ImagingSci.Technol.2017.61.4.040406]

## INTRODUCTION

There are many imperceptible, subtle changes that can be observed. The skin color changes slightly due to blood flow and the heartbeat component on the skin surface can be detected remotely by analyzing dynamic images.[1,2] Clothes also move slightly while sleeping. It is possible to analyze the status of respiration by video analysis.[3] These remote observations of physiological status hold great potential for healthcare applications, medical diagnosis, and affective computing. For example, heart rate variability spectrograms (HRVSs) are useful for remote monitoring of cognitive stress[4,5] and driver awareness,[6] since the HRVS is related to the status of the autonomic nervous system, which controls involuntary body functions such as breathing, blood pressure and heartbeat.

Wu et al. showed that Eulerian video magnification (EVM) can amplify slight changes of facial color and can visualize the blood flow in human faces.[7] Visualization of the blood flow is beneficial to many healthcare and medical applications. Variation of facial blood flow can yield a clue to estimate affective status.[8–10] Detection of the difference in blood flow between the left foot and the right foot can provide useful information for the diagnosis of arteriosclerosis.[11] In surgical procedures, the detection of blood vessels is useful in order to reduce patient damage by preventing bleeding. The blood vessels under the surface are sometimes invisible. In this case, surgeons often estimate the position by referring to anatomical *a priori* knowledge or by relying on sense of touch.

The conventional EVM method shows effectiveness under a stable photographic environment. The subject is required to remain stable in order to avoid illumination changes caused by motion. The conditions of illumination are also required to remain constant during the capture time. This is a limitation for practical use.

In this article, we propose new approach of EVM based on separation of the chromophore component in order to enhance the robustness against illumination changes. Tsumura et al.[12] proposed a method to separate hemoglobin, melanin, and shading components from a skin image captured with a standard RGB camera. The method can extract the hemoglobin component, which varies according to the heartbeat, and the method can eliminate the shading component, which is sensitive to illumination change. Therefore, we apply the separation method to EVM since the method can be expected to enhance the robustness against illumination change.

The rest of this article is organized as follows. In the second section, we describe the proposed EVM based on separation of the chromophore component. In the third section, we show the results of EVM for visualizing blood flow in the human face. In the fourth section, we describe modification of the chromophore component separation for medical application and show the results of EVM using a tongue movie as preliminary work for medical application. In the fifth section, we present our conclusions.

## VIDEO MAGNIFICATION USING SEPARATION OF THE CHROMOPHORE COMPONENT

In this section, we describe the video magnification method based on separation of the hemoglobin component.

### *Eulerian Video Magnification*

The original video magnification method, Eulerian video magnification (EVM),[7] has two kinds of method to amplify subtle changes in video, enhancement of small motion and enhancement of small color change. We aim at enhancement of small color changes in videos. Figure 1 shows an overview

▲ IS&T Members.

Received Mar. 1, 2017; accepted for publication June 19, 2017; published online July 20, 2017. Associate Editor: Henry Y. T. Ngan.
1062-3701/2017/61(4)/040406/7/$25.00

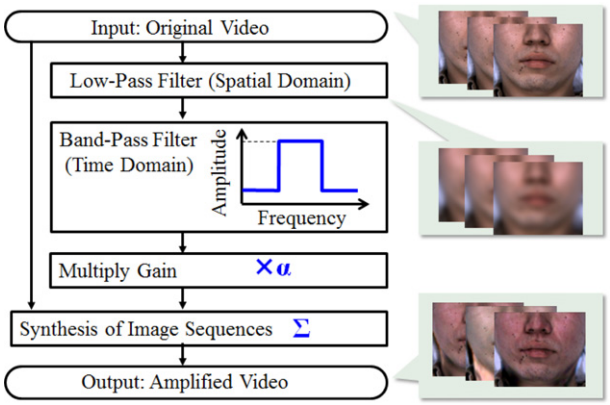


Figure 1. Overview of conventional Eulerian video magnification.

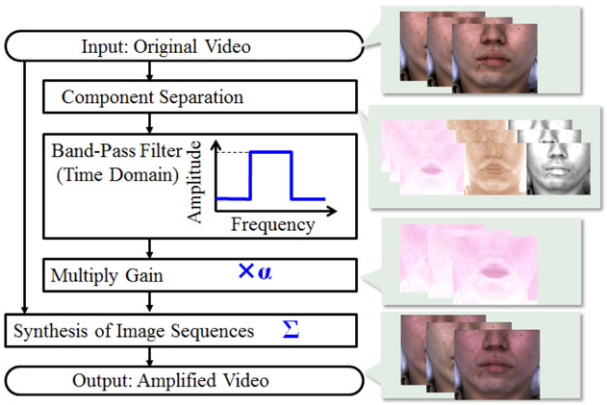


Figure 2. The framework of video magnification for biomedical dynamic images.

of the conventional Eulerian video magnification procedure to amplify subtle color changes. First, the method processes the spatially blurred video frames from the input video frames to reduce locally random noise. Next, a temporal band-pass filter is applied to the blurred video in order to extract the component of temporal color change. Then, the band-passed video frames are synthesized with the original input video frames to multiply the gain factor.

We apply a similar framework to enhance small color changes. Figure 2 shows the framework of the proposed method. We apply a component separation process to extract the hemoglobin component and synthesize it with the original input video frames by multiplying the gain factor. The fluctuation of the hemoglobin component indicates heartbeat behavior and it is free from side effects caused by shading change, which will be described in the next section.

### *Extraction of the Hemoglobin Component*

The technique to extract the hemoglobin chromophore from a single skin color image[12] is briefly reviewed in this subsection.

Figure 3 shows the skin model for the extraction of the hemoglobin component. We use a two-layered skin model composed of epidermis and dermis. We should note

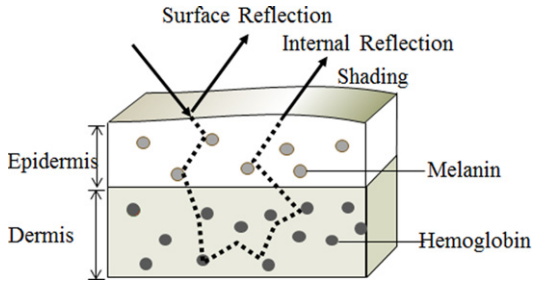


Figure 3. The skin model of the hemoglobin extraction.

that the chromophores of melanin and hemoglobin are predominantly found in the epidermal and dermal layers, respectively. This model was derived from previous research on skin optics.[13–15] The reflected light from the skin surface consists of surface reflection and internal reflection. The internal reflection can be described as follows using the modified Lambert–Beer law,[16] which uses the mean path length of photons in the medium as the depth of the medium:

$$L(x, y, \lambda) = e^{-\rho_m(x,y)\sigma_m(\lambda)l_e(\lambda)-\rho_h(x,y)\sigma_h(\lambda)l_d(\lambda)}E(x, y, \lambda), \tag{1}$$

where $E(x, y, \lambda)$ denotes the spectral irradiance of the incident light at point $(x, y)$; $\rho_m(x, y)$, $\rho_h(x, y)$ denote the concentration, and $\sigma_m(\lambda)$, $\sigma_h(\lambda)$ denote the absorption area of melanin and hemoglobin, respectively; $l_e(\lambda)$, $l_d(\lambda)$ denote the average light path in the epidermis and dermis layer, respectively. By putting polarization filters in front of the illumination and the camera, we can ignore the surface reflection. The camera signal $v_i(x, y)$, $i = R, G, B$, can be modeled as

$$\begin{aligned} v_i(x, y) &= k \int L(x, y, \lambda)s_i(\lambda)\,\mathrm{d}\lambda \\ &= k \int e^{-\rho_m(x,y)\sigma_m(\lambda)l_e(\lambda)-\rho_h(x,y)\sigma_h(\lambda)l_d(\lambda)} \\ &\qquad E(x, y, \lambda)s_i(\lambda)\,\mathrm{d}\lambda, \end{aligned} \tag{2}$$

where $s_i(\lambda)$ denotes the spectral sensitivity of the camera and $k$ denotes the coefficient of camera gain. The spectral reflection of skin is smooth and it is approximately correlated with the camera sensitivity. We assume that $s_i(\lambda)=\delta(\lambda-\lambda_i)$.

We assume that the spectral irradiance of the incident light $\bar{E}(\lambda)$ is uniform over the observation area, and the shading coefficient $p(x, y)$ accounts for the concavity and convexity of the surface. We derive

$$E(x, y, \lambda) = p(x, y)\bar{E}(\lambda). \tag{3}$$

The camera signal $v_i(x, y)$ can be simply rewritten as

$$v_i(x, y) = ke^{-\rho_m(x,y)\sigma_m(\lambda_i)l_e(\lambda_i)-\rho_h(x,y)\sigma_h(\lambda_i)l_d(\lambda_i)}p(x, y)\bar{E}(\lambda_i). \tag{4}$$

By taking the logarithm of both sides of Eq. (4), we derive

$$\boldsymbol{v}^{\log}(x, y) = -\boldsymbol{\rho}_m(x, y)\boldsymbol{\sigma}_m - \boldsymbol{\rho}_h(x, y)\boldsymbol{\sigma}_h + p^{\log}(x, y)1 + \mathrm{e}^{\log}, \tag{5}$$

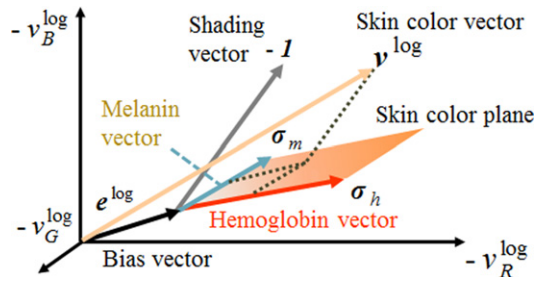


Figure 4. Model of the separation of skin components.

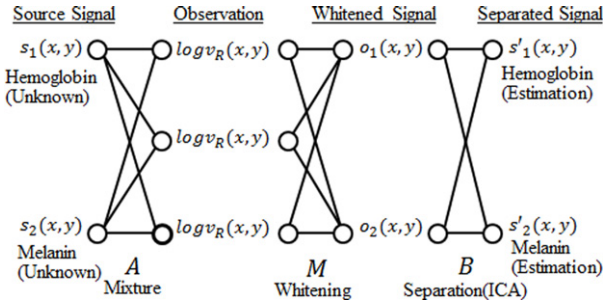


Figure 5. Mixture and separation of independent signals.

(a) hemoglobin (b) melanin (c) shading

Figure 6. Separation result of melanin, hemoglobin, and shading components.

where

$$\boldsymbol{v}^{\log}(x,y) = [\log v_R(x,y) \;\; \log v_G(x,y) \;\; \log v_B(x,y)]^T,$$
$$\boldsymbol{\sigma}_m = [\sigma_m(\lambda_R) l_e(\lambda_R) \;\; \sigma_m(\lambda_G) l_e(\lambda_G) \;\; \sigma_m(\lambda_B) l_e(\lambda_B)]^T,$$
$$\boldsymbol{\sigma}_h = [\boldsymbol{\sigma}_h(\lambda_R) l_d(\lambda_R) \;\; \sigma_h(\lambda_G) l_d(\lambda_G) \;\; \sigma_h(\lambda_B) l_d(\lambda_B)]^T,$$
$$\mathbf{1} = [1 \quad 1 \quad 1]^T,$$
$$p^{\log}(x,y) = \log(p(x,y)) + \log(k),$$
$$\mathbf{e}^{\log}(x,y) = [\log E_R(\lambda_R) \;\; \log E_G(\lambda_G) \;\; \log E_B(\lambda_B)]^T. \quad (6)$$

Here, $v_R(x,y)$, $v_G(x,y)$, $v_B(x,y)$ are the $R$, $G$, $B$ signals at the position $(x,y)$; $\sigma_m(\lambda_R)$, $\sigma_m(\lambda_G)$, $\sigma_m(\lambda_B)$ and $\sigma_h(\lambda_R)$, $\sigma_h(\lambda_G)$, $\sigma_h(\lambda_B)$ are the absorption areas of melanin and hemoglobin for RGB wavelength, respectively; $l_e(\lambda_R)$, $l_e(\lambda_G)$, $l_e(\lambda_B)$ and $l_d(\lambda_R)$, $l_d(\lambda_G)$, $l_d(\lambda_B)$ are the average light paths in the epidermis and dermis layers for RGB wavelength, respectively; $p(x,y)$ indicates the shading coefficient; $k$ denotes the coefficient of camera gain; $E_R(\lambda_R)$, $E_G(\lambda_G)$, $E_B(\lambda_B)$ are the components of spectral irradiance of incident light for RGB wavelength, respectively.

Figure 4 shows the relation between the input RGB signal and each component. The logarithm of the captured RGB signals $\boldsymbol{v}^{\log}$ can be represented by the weighted linear combination of four vectors, the melanin vector $\boldsymbol{\sigma}_m$, the hemoglobin vector $\boldsymbol{\sigma}_h$, the shading vector $\mathbf{1}$, and the bias vector $\mathbf{e}^{\log}$.

We predefine a skin color plane using a training data set. Figure 5 shows the mixing and separation process of the melanin and hemoglobin signals for definition of the skin color plane. Let us denote by $\boldsymbol{A} = [\boldsymbol{a}_1, \boldsymbol{a}_2]$ the constant $3 \times 2$ mixing matrix and by $\mathbf{s}(x,y) = [\mathbf{s}_1(x,y), \mathbf{s}_2(x,y)]^T$ the quantity vector on the image coordinates $(x,y)$. Now, $\boldsymbol{v}^{\log}(x,y)$, the logarithm of the observational RGB signals, can be written as follows:

$$\boldsymbol{v}^{\log}(x,y) = \boldsymbol{A}\mathbf{s}(x,y). \quad (7)$$

If the mixing matrix $\boldsymbol{A}$ is known, we can obtain an estimation of the source signal $\mathbf{s}'(x,y)$ using the separation matrix $\boldsymbol{H}$ as follows:

$$\mathbf{s}'(x,y) = \boldsymbol{H}\boldsymbol{v}^{\log}(x,y), \quad (8)$$

where $\boldsymbol{H} = \boldsymbol{A}^{-1}$. However, $\boldsymbol{A}$ is usually unknown. Hence, we create a whitened signal $\boldsymbol{o}(x,y) = [o_1(x,y), o_2(x,y)]^T$ whose elements $o_1(x,y)$ and $o_2(x,y)$ are mutually uncorrelated by applying a whitening process to the source quantity vector $\mathbf{s}(x,y) = [\mathbf{s}_1(x,y), \mathbf{s}_2(x,y)]^T$, and we obtain an estimation of the source signal $\mathbf{s}'(x,y) = [\mathbf{s}'_1(x,y), \mathbf{s}'_2(x,y)]^T$ using independent component analysis (ICA). This process can be rewritten as follows:

$$\mathbf{s}'(x,y) = \boldsymbol{H}\boldsymbol{v}^{\log}(x,y) = B\boldsymbol{M}\boldsymbol{v}^{\log}(x,y), \quad (9)$$

where the whitening matrix is $\boldsymbol{M}$ and the separation matrix by ICA is $B$.

In this case, the number of observational signals is three, RGB, whereas the number of original source signals is two, melanin and hemoglobin. We reduce the dimension of the observation using principal component analysis and define a skin color plane that contains the first principal component and the second principal component. This process is the same as the whitening process.

We predefine a skin color plane using a training data set. The logarithm of the captured RGB signals $\boldsymbol{v}^{\log}$ is projected onto the skin color plane along with the shading vector $\mathbf{1}$. From the position on the skin plane, we obtain the hemoglobin vector. Figure 6 shows an example of the result of melanin, hemoglobin, and shading components.

## EVALUATION OF BLOOD FLOW IN THE HUMAN FACE

In this section, we show the experimental results of video magnification to visualize blood flow using the extracted hemoglobin component in the human face.

The camera used to collect the video sequences for analysis was a Point Grey Grasshopper3 (GS3-U3-23S6C-C). The frame rate was 60 [fps], each video frame was $928 \times 760$ [pixels], 12 bit RAW format, no compression. The lens was a Fujinon DF6HA-1B, F1.2, focus length 6 mm. The distance of the subject from the camera was 1.0 m. The

(a) Original Video (consecutive frames)

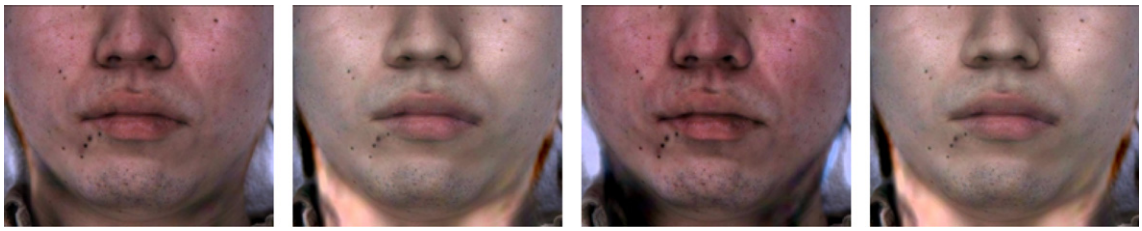

(b) Conventional Method: Eulerian Video Magnification [7]

(c) Proposed Method: Video magnification Using Estimation of the Chromophore Component

Figure 7. Video magnification to visualize blood flow in the human face. (a) Four frames from the original video sequence (face). (b) The same four frames with the subject's pulse signal amplified using the conventional method.[7] (c) The same four frames with the subject's pulse amplified using the proposed method.

illumination, an artificial solar light (SOLAX XC-100), was used from a distance of 1.0 m.

Figure 7 shows the experimental results of video magnification to visualize blood flow in the human face. The conventional method,[7](b), and the proposed method, (c), used magnification with a gain of 50. The original video sequence, (a), does not show a pulse signal between the four frames. The conventional method, (b), amplifies the pulse signal in the subject's face. However, the frames have a black line along the neck as an undesirable artifact. The result shows that the conventional method mistakenly amplifies the shading component since it simply amplifies the pixel values of the blurred image. On the other hand, the proposed method, (c), amplifies the pulse signal in the subject's face without having clear artifacts. The results show that the proposed method can successfully eliminate the shading component in the chromophore separation process and effectively enhance the pulse signal by amplifying the hemoglobin component.

## PULSE DETECTION FOR MEDICAL APPLICATION

In this section, we describe the modification of chromophore component separation for medical application and show the results of video magnification using a tongue movie as preliminary work for a medical application.

For the pulse detection in the facial area, which is described in the second section, we extract the hemoglobin component by utilizing a two-layered skin model consisting of melanin and hemoglobin. In this section, we also utilize a similar approach for pulse detection from medical videos. However, the surfaces of the epithelium do not have melanin chromophores. We cannot utilize the skin color plane shown in Fig. 4 in order to extract the hemoglobin component from medical images. Figure 8 shows the temporal behavior of the hemoglobin component in the facial region and the back of tongue, which is extracted using the skin color plane in Fig. 4.

The temporal behavior of the back of the tongue does not show a pulse when we use the skin color plane, whereas the method works well in the facial area. This is because the separation method described the second section is designed for the separation of melanin, hemoglobin, and shading components for skin.

It is known that the combination of two illumination wavelengths, 415 nm and 540 nm, is effective for endoscopes to visualize blood vessels under the surface of the epithelium.[17,18] Hence, we make a hypothesis that we can simply represent the existence of blood vessels using the mixture model of two substances. We collect images of the back of the tongue on vessels and off vessels, respectively, and define a tongue color plane that contains the first and second principal components, as described in Figure 9. The basic

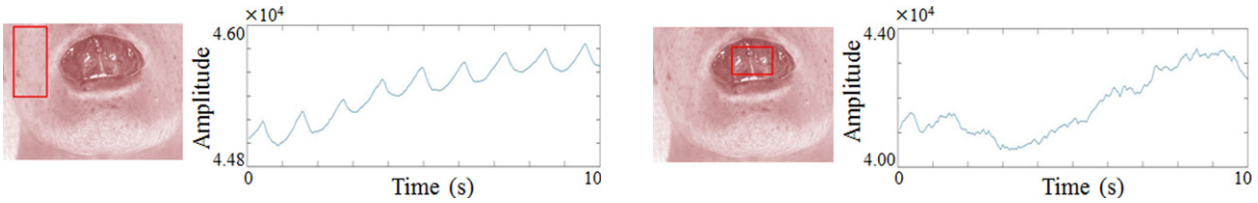


(a) Hemoglobin Component in skin area

(b) Hemoglobin Component on the back of tongue

Figure 8. Behavior of the hemoglobin component. (a) Skin area. (b) Back of tongue.

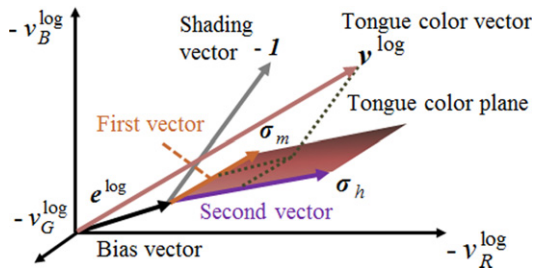


Figure 9. Model to separate components on the back of the tongue.

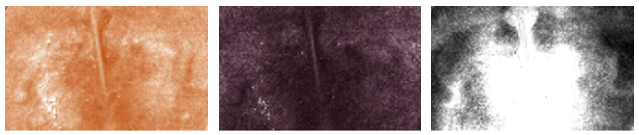

(a) First Vector Component

(b) Second Vector Component

(c) Shading Component

Figure 10. Estimation result of components on the back of the tongue.

framework of the separation of chromophores is same as skin component separation. Figure 10 shows an example of the separation of tongue components.

Figure 11 describes the experimental results of the video magnification using a tongue movie. The conventional method,[7](b), amplifies the blurred image with gain 50. The proposed method, (c), amplifies the first independent component on the tongue color plane with gain 50. The original video sequence, (a), does not show a pulse signal between the four frames. The conventional method, (b), shows variation of an undesirable dark region in each frame. The result indicates that the conventional method mistakenly amplifies the shading component since it simply amplifies the pixel values of the blurred image. On the other hand, the proposed method, (c), shows the periodical color variation on the surface of the vessel without any artifacts. This indicates that the proposed method amplifies a specific independent component which is correlated with blood flow by eliminating the shading component.

Figure 12 shows the pulse distribution in the tongue region. In the red region, the wave of the first independent component on the tongue color plane shows periodical variation which corresponds to the pulse signal, (c). Therefore, there is a sharp peak around 1 Hz (60 bpm: beat per minute) in frequency analysis by Fast Fourier Transform (FFT). On the other hand, in the green region, the wave of the first independent component does not show periodical variation, (d). Hence, the frequency peak around 1 Hz (60 bpm) is lower than that of the red region. We utilize this property to visualize the distribution of the pulse signal. The heat map, (b), shows the distribution of the pulse signal, which is calculated by taking the sum of the magnitude of the frequency component from 1 Hz (60 bpm) to 1.4 Hz (71 bpm). It is useful to observe the detailed distribution of the pulse component more than the video magnification.

## CONCLUSION AND DISCUSSION

In this article, we propose a novel method of video magnification based on separation of the chromophore components. Using the test video data, we confirm that the proposed method can visualize blood flow in the human face without artifacts caused by shading change. We also apply the video magnification framework to a tongue movie as preliminary work for medical application. We define the tongue color plane by ICA and we use the first component for video magnification after confirming that the first component shows the periodical behavior caused by blood pulses. We also confirm the effectiveness of video magnification using the first component of ICA. It can enhance blood flow, avoiding the artifacts caused by shading change. Furthermore, we propose a heat map format to show the detailed distribution of blood flow by analyzing the magnitude of the frequency component of the pulse wave.

Finally, we mention the current limitations and future work. First, we evaluated a small number of samples to examine the effectiveness as preliminary work. An evaluation with a large number of samples is necessary for future work. Second, we also have to think about how to assess the performance. In this article, we evaluate the effectiveness of the enhancement of blood flow with eyes. We have to think about a method to access the performance quantitatively. Third, we have to study the scientific evidence of the two mixture models for a medical application. The effectiveness of the skin model has been evaluated previously.[12,19] However, the mixture model for medical application is based on a hypothesis from the knowledge of Refs. 17, 18. It is important to confirm and evaluate the scientific evidence. This might lead to optimization of the illumination spectra. Fourth, we also have to confirm the effectiveness for detection of blood vessels on the

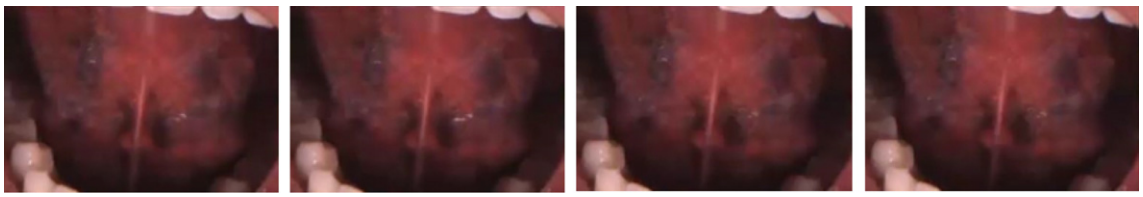

(a) original video (consecutive frames)

(b) The results of previous method: Eulerian Video Magnification

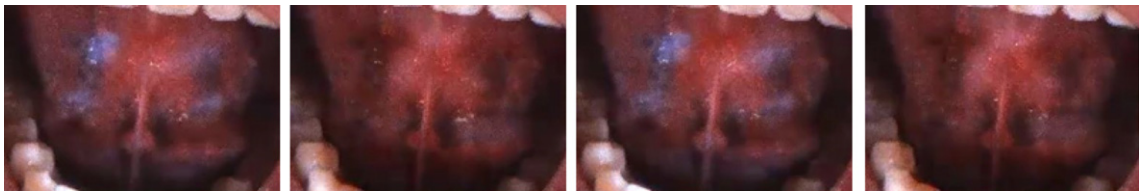

(c) The results of proposed method: video magnification using pigment component separation

Figure 11. Video magnification to visualize blood flow on the back of the tongue. (a) Four frames from the original video sequence (back of tongue). (b) The same four frames with the pulse signal amplified using the conventional method.[7] (c) The same four frames with the pulse amplified using the proposed method.

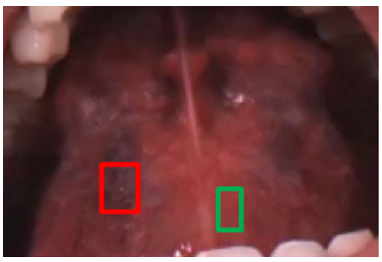

(a) Original Video

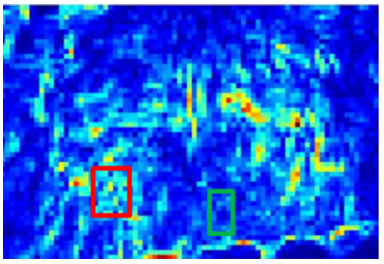

(b) Heat Map to Indicate Blood Flow

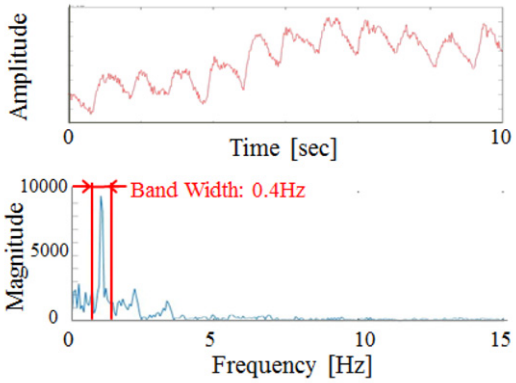


(c) First Vector Component and its Frequency Analysis (Red Region)

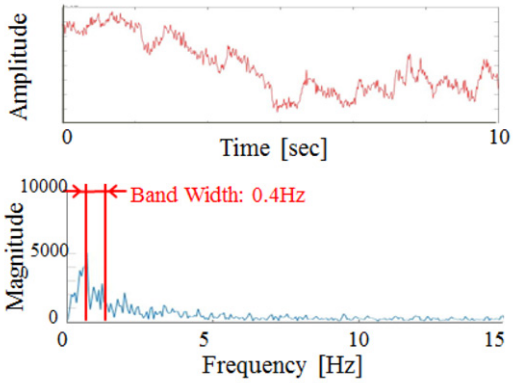


(d) First Vector Component and its Frequency Analysis (Green Region)

Figure 12. The distribution of pulse intensity. (a) Original video frame. (b) Heat map of the pulse intensity. (c) First vector component and its frequency analysis (red region). (d) First vector component and its frequency analysis (green region).

medical front. As a next step, we also have to study the usability of switching between the usual observation and the enhanced mode that we proposed at this time. Fifth, real time processing also remains for future work. Currently, the processing is carried out by Matlab code after taking a video sequence. Thinking about implementation as a product,

hardware processing such as ASIC is necessary for real time processing.

## REFERENCES


[1] M.-Z. Poh, D. J. McDuff, and R. W. Picard, "Non-contact, automated cardiac pulse measurements using video imaging and blind source separation," Opt. Express **18**, 10762–10774 (2010).

[2] M.-Z. Poh, D. J. McDuff, and R. W. Picard, "Advancements in noncontact, multiparameter physiological measurements using a Webcam," IEEE Trans. Biomed. Eng. **58**, 7–11 (2011).

[3] D. Shao, Y. Yang, C. Liu, F. Tsow, H. Yu, and N. Tao, "Noncontact monitoring breathing pattern, exhalation flow rate and pulse transit time," IEEE Eng. Med. Biol. Soc. **61**, 2760–2767 (2014).

[4] D. McDuff, S. Gontarek, and R. W. Picard, "Improvements in remote cardio-pulmonary measurement using a five band digital camera," IEEE Trans. Biomed. Eng. **61**, 2593–2601 (2014).

[5] K. Kurita, T. Yonezawa, M. Kuroshima, and N. Tsumura, "Non-Contact video based estimation for heart rate variability spectrogram using ambient light by extracting hemoglobin information," *Proc. IS&T CIC23: Twenty-third Color and Imaging Conf.* (IS&T, Springfield, VA, 2015), pp. 207–211.

[6] G. Li and W. -Y. Chung, "Detection of driver drowsiness using wavelet analysis of heart rate variability and a support vector machine classifier," Sensors **13**, 16494–16511 (2013).

[7] H. -Y. Wu, M. Rubinstein, E. Shih, J. Guttag, F. Durand, and W. Freeman, "Eulerian video magnification for revealing subtle changes in the world," ACM Trans. Graph. **31**, 1–8 (2012).

[8] P. D. Drummond and S. H. Quah, "The effect of expressing anger on cardiovascular reactivity and facial blood flow in Chinese and Caucasians," Psychophysiol. **38**, 190–196 (2001).

[9] N. Hayashi, N. Someya, T. Maruyama, Y. Hirooka, M. Yamaoka-Endo, and Y. Fukuba, "Vascular responses to fear-induced stress in humans," Physiol. Behav. **98**, 441–446 (2009).

[10] G. Okada, T. Yonezawa, K. Kurita, and N. Tsumura, "Emotion monitoring using remote measurement for physiological signals by camera," *Proc. IS&T CIC24: Twenty-four Color and Imaging Conf.* (IS&T, Springfield, VA, 2016), pp. 147–151.

[11] P. Kunkel and E. A. Stead Jr., "Blood flow and vasomotor reactions in the foot in health, in arteriosclerosis, and in thromboangiitis obliterans," J. Clin. Invest. **17**, 715 (1938).

[12] N. Tsumura, N. Ojima, K. Sato, M. Shiraishi, H. Shimizu, H. Nabeshima, S. Akazaki, K. Hori, and Y. Miyake, "Image-based skin color and texture analysis/synthesis by extracting hemoglobin and melanin information in the skin," ACM Trans. Graph. **22**, 770–779 (2003).

[13] R. R. Anderson and J. A. Parrish, "The optics of human skin," J. Investigate Dermatology **77**, 13–19 (1981).

[14] M. J. V. Van Gemert, S. L. Jacques, H. J. C.M Sterenborg, and W. M. Star, "Skin optics," IEEE Trans. Biomed. Eng. **36**, 1146–1154 (1989).

[15] N. Tsumura, M. Kawabuchi, H. Haneishi, and Y. Miyake, "Mapping pigmentation in human skin from multi-channel visible spectrum image by inverse optical scattering technique," J. Imaging Sci. Technol. **45**, 444–450 (2001).

[16] M. Hiraoka, M. Firbank, M. Essenpreis, M. Cope, S. R. Arridge, P. van der Zee, and D. T. Delpy, "A Monte Carlo investigation of optical pathlength in inhomogeneous tissue and its application to near-infrared spectroscopy," Phys. Med. Biol. **38**, 1859–1876 (1993).

[17] K. Gono, T. Obi, M. Yamaguchi, N. Ohyama, H. Machida, Y. Sano, S. Yoshida, Y. Hamamoto, and T. Endo, "Appearance of enhanced tissue features in narrow-band endoscopic imaging," J. Biomed. Opt. **9**, 568–577 (2004).

[18] https://www.olympus-europa.com/medical/en/medical_systems/applications/urology/bladder/narrow_band_imaging_nbi_/narrow_band_imaging_nbi_.html.

[19] K. Kurita, T. Yonezawa, and N. Tsumura, "Non-contact video based estimation for heart rate variability spectrogram using ambient light by extracting hemoglobin information," *Proc. IS&T CIC23: Twenty-third Color and Imaging Conf.* (IS&T, Springfield, VA, 2015), pp. 207–211.